Chapter 2

A compact and lens less digital holography setup for polarimetric analysis of spatial light modulator

2.1 Introduction

Digital holography (DH) is a rapidly developing area that has gained significant attention due to its potential to capture and reconstruct three-dimensional (3D) images by providing intensity and phase information simultaneously. The advantages of the DH-based methods lie in their ability to provide quantitative information. DH can be performed using different configurations, i.e., in-line, off-axis, and phase shifting as explained in chapter 1. An in-line holography records the interference of a diffracted and non-diffracted light emerging out of the sample. This technique is stable but suffers from a twin image problem. Several methods have been proposed to avoid the twin-image problem in recent years. Off-axis configuration is another significant method employed in the DH. This technique uses a reference and the object beams with a suitable angular separation to avoid the twin image issue. The advantage of off-axis holography lies in its ability to offer quantitative

images from a single intensity measurement and without iterations. However, a major issue associated with the off-axis DH is the stability due to separate paths for object and reference beams. Therefore, any mechanical vibration or disturbance can have distinct effects on the two interference beams. Moreover, it demands many optical components in the experimental set-up and thus causes strict stability constraints in the experimental implementation. Various studies have been reported to address the stability issues in the DH. Recently interferometric systems based on common paths have been widely used and are claimed to enhance the stability of corresponding experimental methods. In common path interferometry, the reference beam and object beam are allowed to traverse nearly the same optical paths. Therefore, common path interferometry systems are stable and offer new alternatives on the DH designs. These common-path configurations are compact and robust and are also advantageous in optical instrument manufacturing. The main challenge in designing a common-path setup is to make a common path for the object and reference and yet insert the object in one of the interfering arms. A few useful common path interferometric designs are discussed below. The common path DH design can be realized by various methods, such as using a trapezoid Sagnac-interferometer [55], a glass plate [56], grating [57], etc. In the optical design developed by Ma et al [55], a polarised BS (PBS) splits the object beam into two counter-propagating components with orthogonal polarisation states. These two orthogonal components travels through the similar optical elements as shown in Fig. 2.1. One of the beams carries sample information and other propagates without any object information. These two interference beams are recorded at the CCD plane. Other specialised optical elements can also be used in the lateral shearing-based common-path configurations to create compact and stable holographic experimental setups, such as the beam displacer [58], Wollaston prism [59], and biprism [60] etc.

Another interesting approach rely on deriving a reference beam from the object information by using a pinhole filtering prior to the interference [16, 17, 61, 62]. An on-axis

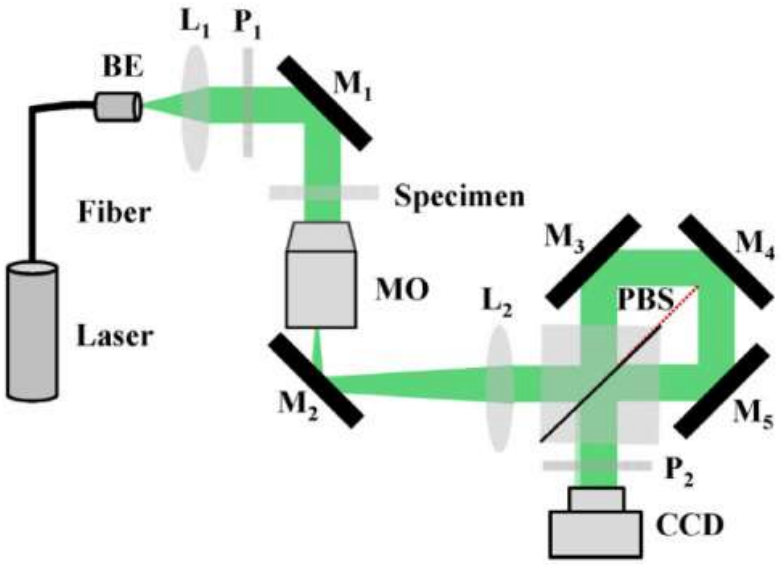

Fig. 2.1 Experimental setup of the common-path digital holography based on a slightly trapezoid Sagnac interferometer [55]

interferometer called as τ interferometer uses two beams traveling equal paths, and one of the beams spatially filtered by a pinhole is used as a reference beam as shown in Fig. 2.2 [16, 61].

The majority of the aforementioned DH techniques account the scalar nature of the light wherein the polarization parameter of the light is ignored. On the other hand, polarization is a vital characteristic of light to reveal the structural information of the object. The DH can be extended to record and reconstruct the complete wavefront of the light, i.e. amplitude, phase, and polarization [12, 19, 20, 63, 64]. The DH to extract polarization feature of the coherent light, called polarization digital holography (PDH), is possible by recording and reconstructing the orthogonal polarization components of the light. The PDH is expected to play significant role in the characterization of polarization devices/elements and one such important device is the SLM. Programmable feature of the SLM is widely used in modulating amplitude, phase, and polarization of light. The SLM is deployed as a dynamic device in applications such optical tweezers [65], beam shaping [66], coded

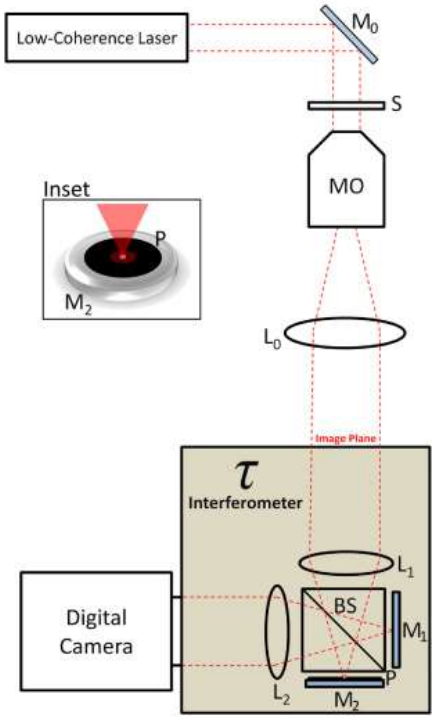

Fig. 2.2 Experimental setup of the τ interferometer fitted into the output of an inverted microscope [16]

aperture [67] etc. SLMs are liquid crystal (LC) based devices where the rotation of LC molecules with respect to the addressed pixel voltage (gray values) provides the required phase modulation for the SLM. Moreover, the SLMs are sensitive to the polarization of the incident light. It can modulate the state of polarization (SOP) of incident light with respect to its gray values. The modulation characteristics of SLM are compromised due to limited fill factor, non-active area, edge diffraction [68, 69] etc. Therefore, a robust calibration of the SLM is required prior to its utilization in applications Several studies have been reported to characterize the phase modulation characteristics of the SLM such as using self-referencing common-path interferometer [70], self-referenced multiple-beam interferometric design [71], using iterative algorithms [72], diffraction-based phase calibration [73], geometric phase interferometry [74], measuring Jones matrices [75, 76]. SLM characterization techniques can be divided into two categories, i.e. interferometric

techniques [70, 71, 72, 73, 74, 77, 78] and polarimetric techniques [75, 76, 79, 80, 81, 82]. In interferometric techniques, the phase modulation of the SLM is calibrated from the multiple recorded interference patterns by observing the relative fringe shift. Advantages of the interferometric approach lie with its ability to extract coherent information of the light and also apply the digital back propagation. However, these interferometers usually require an additional reference beam and hence sensitive to vibrations [18]. Gao et al. proposed a self-referenced interferometric technique for calibration of SLM [71]. On the other hand, the polarimetric techniques for LC-SLM characterization are based on the relative phase shift between two orthogonal states of polarization (SOPs) of light [76]. Recently, an off-axis holographic imaging technique is proposed to calibrate the SLM and extract complete polarimetric information using the coherent light [75]. This technique employs a Mach-Zhender interferometer with tuned carrier frequencies for the spatially multiplexed orthogonally polarized reference beams. In situ calibration method based on DH to calibrate the spatial non uniformity of the phase modulation of phase only SLM is demonstrated. The technique rely on dividing the SLM screen into different blocks of pixels and the differential phase of those blocks can be reconstructed using the DH [83]. A technique using diffractogram analysis with stable configuration has also been used in past for the calibration of phase only SLM [84].

In this chapter, we present and experimentally demonstrate a new approach for complete polarimetric analysis of the SLM. Our experimental system uses a compact cyclic Sagnac interferometer along with a residual de-collimated beam for the illumination. This interferometer consists of two mirrors and a beam splitter. The two counter propagating light beams in the interferometer traverse nearly a similar optical path and therefore offer a high stability even in the external vibrating conditions. We apply a strategy to use a half portion of the field illumination to insert the SLM characteristics and remaining half portion of the incident beam is untouched. Use of the spherical wave illumination and the

lateral shearing by our cyclic interferometer helps to encode the polarimetric characteristics of the SLM into the fringes. These fringes with varying gray levels are subjected to digital reconstruction for complete recovery of the wavefronts. A polarization characteristic of the SLM is evaluated with respect to varying gray levels ranging from 0-255 in steps of 5 and examined in different vibrating conditions. Advantages of our technique lies with its ability to fully characterize the polarimetric features of the SLM even in the vibrating conditions and polarimetric phase of the system is nearly same as with the interferometer working on the vibration isolation condition. In comparison to other commonly used interferometric schemes such as Michelson and Mach Zhender, our proposed experimental geometry is highly stable, compact and uses a nearly common path geometry. Detailed theoretical basis, experimental implementation and stability analysis of our technique are presented below.

2.2 Methodology

The experimental setup used for the polarimetric characterisation of TNLC-SLM (LC-R720 model manufactured by HOLOEYE) is shown in Fig. 2.3(a). A monochromatic vertically polarized light beam (He–Ne laser, Edmund optics, 1135 P, λ = 632.8nm) is spatially filtered, and is made to pass through a convex lens L with focal length 150mm which is slightly displaced from the focal length to generate a spherical wave. This spherical wave passes through a half-wave plate (HWP) to generate a 45 degree linearly polarized light. A 50-50 beam splitter (BS1) splits the incoming light into two parts; one part gets reflected and goes to the SLM, and the transmitted beam is dumped. This SLM model has a 45 degree twisted nematic LC layer which alters reflected polarization according to the gray levels displaced on the SLM [75]. The light beam of size 10mm is reflected from the SLM and propagates back to the BS1 and then folded towards a cyclic interferometer composed of a beam splitter (BS2) and two mirrors M1 and M2. The mirrors M1 and M2 are

positioned in such a way that the two beams coming out of the BS2 are laterally separated and propagate towards the charge coupled device (CCD) plane. Different spatial carrier frequencies can be produced by introducing spatial separation of the two beams using the cyclic interferometer assembly. In general, most of the interferometric techniques require a collimating input beam and a separate reference beam. The proposed experimental geometry employs a residual de^collimation strategy to adjust a spatial frequency in the cyclic setup. The amount of de-collimation along with a lateral shearing is used to tune the number of fringes in the recording of the interferogram for the quantitative reconstruction [18]. This experimental strategy along with a de-collimation beam offers a high stability, compactness, and ability to tune the frequency for the quantitative phase retrieval. Fig. 2.3 (b) highlights a flow chart describing the digital reconstruction steps used in the reconstruction of interferograms and digital back propagation of the coherent light to the SLM plane. In order to implement this setup in the polarization domain, a polarizer (P) is placed before the CCD. A laboratory picture of the experimental design is shown in Fig. 2.3 (c). The interference patterns are recorded for two orthogonal components (E_x and E_y) by changing the orientation of polarizer P. The orthogonal polarization fields coming out of the cyclic interferometer is recorded at the CCD plane in two steps. A schematic of the proposed configuration is given in Fig 2.4 (a). Two beams coming out from the BS2 generate an interference pattern which is recorded by the CCD with a pixel resolution 2200×2752 and pixel size 4.54 μm (Procilica, GT-2750). The paths of the two counter propagating beams in the cyclic interferometer are nearly same and hence path length different is significantly smaller than the coherence length of the laser source used in the experiment. This leads to the formation of clear and high contrast interference fringes. Distance between the SLM and recording plane (CCD) is 510 mm in a lens-less geometry. The interference pattern for orthogonal electric field components is represented as,

$$I_x(r) = |R(r) + E_x(r)|^2 \tag{2.1}$$

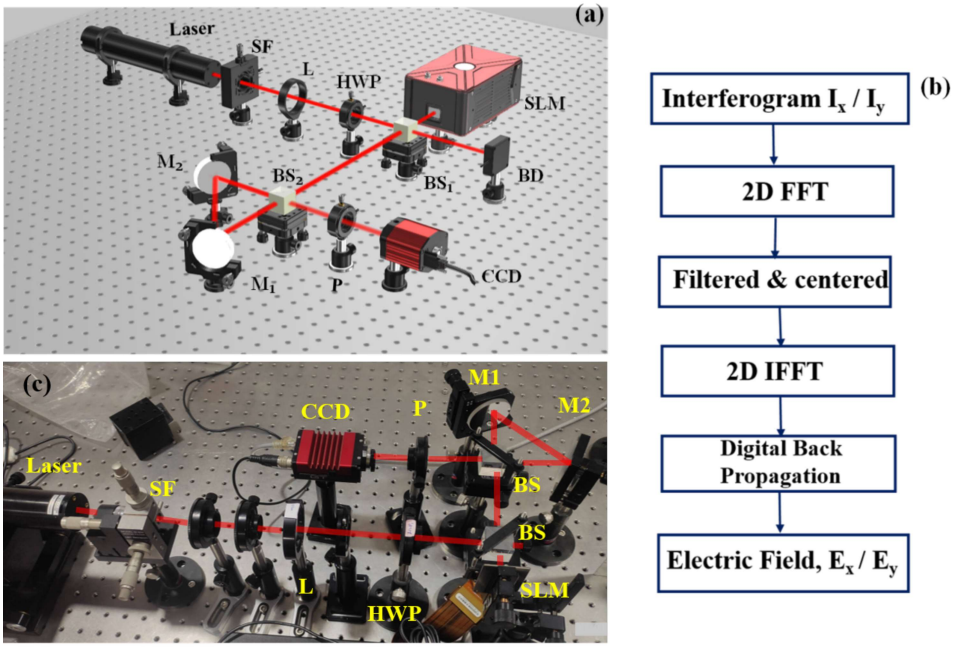

Fig. 2.3 (a) Schematic of the experimental technique. (b) Flowchart for the processing of Interferograms [P: polarizer, HWP: Half wave plate, SF: Spatial filter, L: lens, SLM: Spatial light modulator, BSn(n=1, 2): beam splitters, Mn (n=1, 2): mirrors, CCD: Charge coupled device, BD: Beam dump]. (c) Laboratory picture of experimental design.

$$I_y(r) = |R(r) + E_y(r)|^2 \tag{2.2}$$

where, $r(x,y)$ is a two-dimensional position vector at the CCD plane, I_x and I_y are interference patterns due to orthogonal polarization components oriented along x and y directions, respectively. Terms $E_x(r)$ and $E_y(r)$ represent the orthogonal polarization components of the light, and $R(r)$ is a diverging spherical reference beam. Due to a large propagation distance from the SLM to the camera plane, we considered denominator term of the spherical wave function as a constant factor and ignored it in the representation of the spherical waves. Therefore, a reference wave $R(r)$ coming from the point source (x_1, y_1) is represented as

$$R(r_1) = exp(ikr_1) \tag{2.3}$$

where, $r_1 = \sqrt{(x-x_1)^2 + (x-x_1)^2 + z^2}$

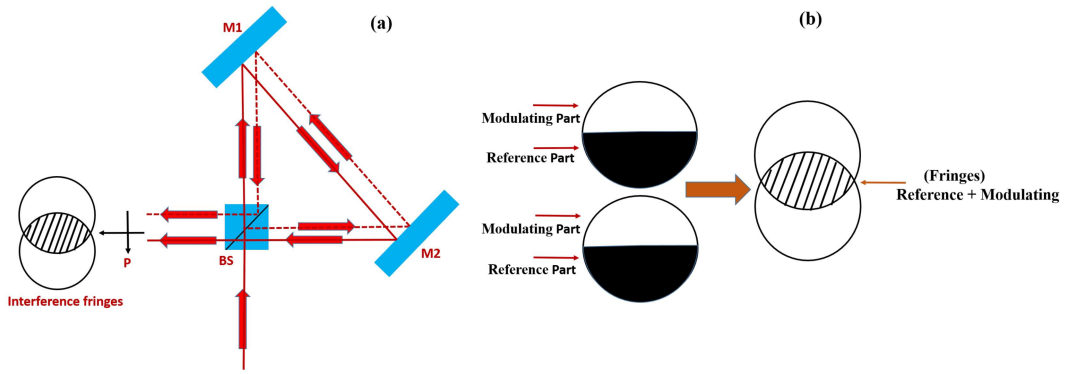

Fig. 2.4 Schematic of the proposed cyclic interferometer and corresponding interferogram (b) Fringe formation from reference and modulating part of SLM screen.

k is wave number and z is longitudinal propagation distance from point source to CCD. On the other hand, the divergent spherical wave from a point source (x_2, y_2) that creates the wavefront of the object wave $O_i(r_2)$ due to the SLM is represented as,

$$E_i(r_2) = O_i(r_2) exp(ikr_1) \tag{2.4}$$

where, $r_2 = \sqrt{(x-x_2)^2 + (x-x_2)^2 + z^2}$ and $i = x, y$ represents the orientation of orthogonal polarization components. In order to perform polarimetric characterization of the SLM with different gray levels, we divided the SLM screen (1280 × 768 pixels) into two parts, i.e., a reference and a modulating part. A reference region is provided a fixed 'zero' gray value and the modulating region is loaded with varying gray levels ranging from 0 to 255 in the steps of 5. Strategy to insert the SLM modulation and subsequent generation of the interference pattern is sketched in Fig. 2.4(b). For a linearly polarized incident with 45-degree orientation, we recorded interference pattern at different gray levels for x and y orthogonal polarization components. The recorded interferograms are then digitally reconstructed using the Fourier fringe analysis to recover the complex fields of the polarization components [18]. Digital back propagation algorithm is applied to retrieve the complex fields at the SLM plane.

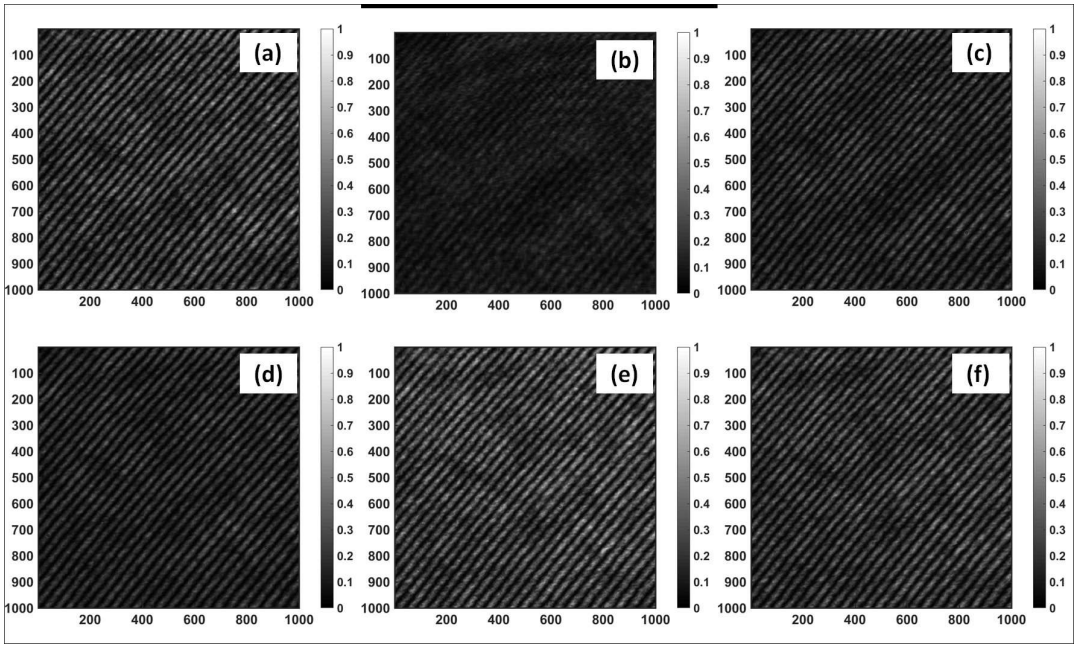

Fig. 2.5 Recorded interference patterns for E_x component (a-c) and for E_y component (d-f) at gray values 5, 180 and 255 for SLM with 45 degree linearly polarized incident light

2.3 Results and Discussion

The light beam propagating through triangular geometry is detected by a camera of limited pixels (2200 × 2752) with a pixel pitch of 4.54 m, i.e., 9.99mm × 12.49mm of detection area. Out of this detection area, the interference fringes of size 8.1mm × 6.1mm are formed within the shearing region as shown in Fig.2.4 (a) and (b), and we used only the central square region of 1000 ×1000 pixels from this interference pattern for the processing of desired complex field with gray levels. Fig. 2.5 (a-c) & 2.5 (d-f) represent the used interference patterns for the reconstruction of the orthogonal polarization components E_x and E_y at gray levels 5,180 and 255 of the SLM respectively. Corresponding Fourier spectra are shown in Figs. 2.6 (a-c) and 2.6 (d-f), respectively. The central frequency region (DC) is suppressed to highlight the off-axis Fourier peaks, as shown with a white circle in Fig. 2.6. These two peaks represent the Fourier spectrum of the electric field component and its conjugate term. A magnified portion of the desired Fourier spectra are

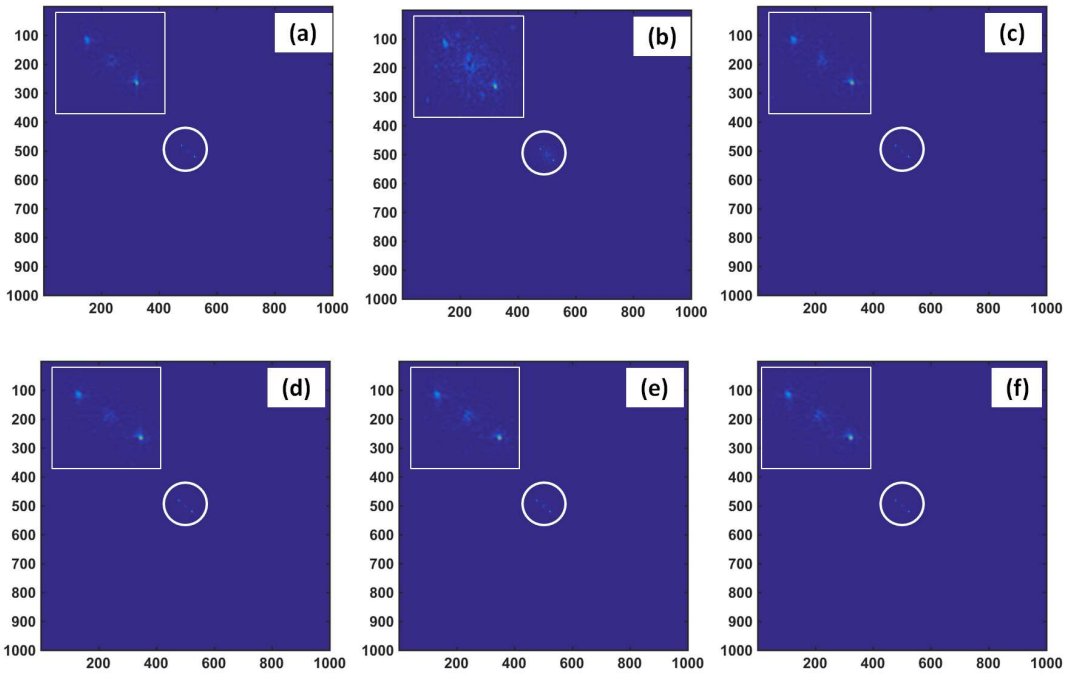

Fig. 2.6 Fourier spectrum for E_x component (a-c) and for E_y component (d-f) at gray values 5, 180, and 255 of SLM with 45 degree linearly polarized incident light. Fig. in the inset represents the highlighted Fourier spectrum).

shown in Fig. 2.6 at the top left in each figure. The retrieved complex field components are obtained at the CCD plane and back propagated to the SLM plane using the angular spectrum method [7]. In order to examine the detailed polarization characteristics of the SLM, we present amplitude and phase distributions of the orthogonal field components with varying gray levels. Back propagated complex field components (at the SLM plane) is represented in Fig. 2.7. Fig. 2.7(a-c) and Fig. 2.7(d-f) represent amplitude for E_x and E_y components at the SLM plane with gray values 5,180 and 255, respectively, whereas Fig. 2.7(g-i) and Fig. 2.7(j-l) represent the phase of E_x and E_y components at the SLM plane with gray values 5,180 and 255 respectively. These results are obtained by performing the experiment on passive vibration isolation table.

Quantitative profiles of the amplitude and phase values with varying gray values are shown in Fig. 2.8. Fig. 2.8 (a) and Fig. 2.8 (b) represent the amplitude and phase

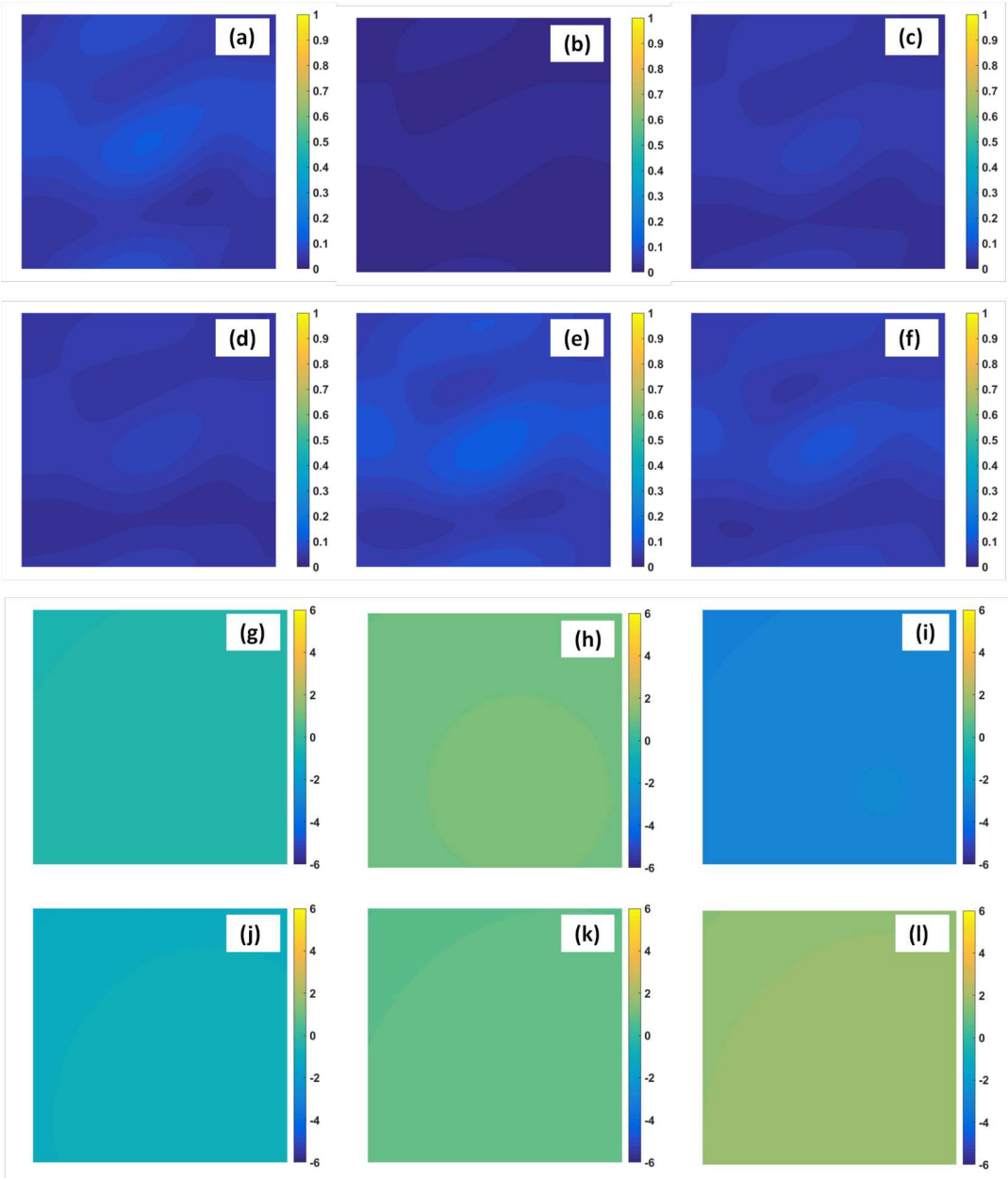

Fig. 2.7 Amplitude distribution for E_x component (a-c); for E_y component(d-f). Phase distribution (ϕ_x) for E_x component (g-i), at gray values 5, 180 and 255 of SLM with 45 degree linearly polarized incident light.

modulation characteristics of the E_x component. It is observed that the amplitude of E_x shows a descending trend up to mid gray value range of the SLM and then gradually increasing up to gray value 255. Similarly, Fig. 2.8 (c) and 2.8 (d) provide the amplitude

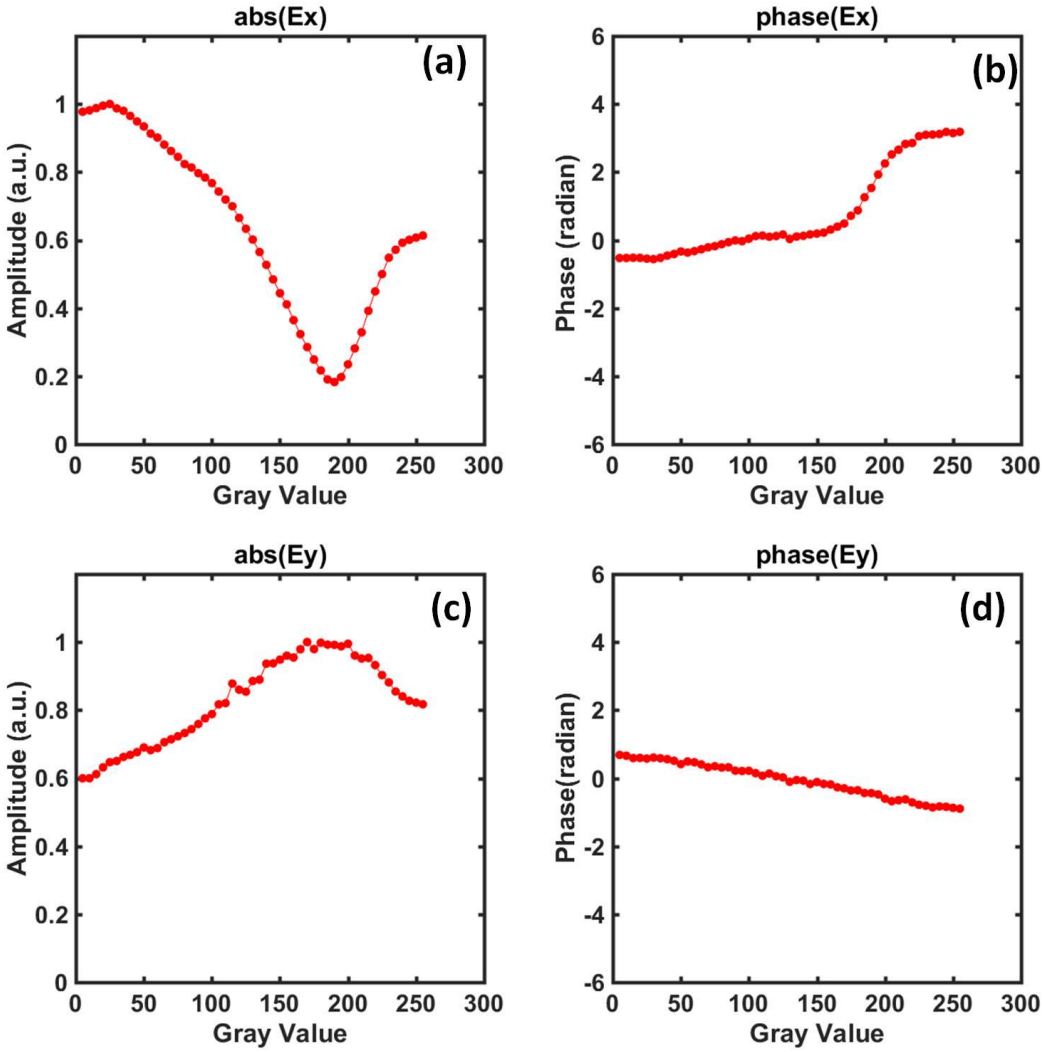

Fig. 2.8 Amplitude and phase modulation curve for incident 45 degree linearly polarized light. Amplitude and phase curve corresponding to field component E_x : (a) & (b) ; amplitude and phase curve corresponding to field component E_y : (c) & (d).

and phase modulation characteristics corresponding to E_y component. The amplitude variation of E_y attains its peak at mid gray values and then reduces gradually. In order to

further test and demonstrate stability of our experimental technique, experiment was again performed in the presence of external vibrations and complete characterization process as mentioned earlier was repeated in the new experimental condition. External vibrations were generated with cell-phone (vibrator motor model: ET-PART-34707-146814) which was placed in the vicinity of our experimental setup at the table and polarimetric analysis of the SLM was carried out with gray values ranging from 0-255 in step of 5. Corresponding results are shown in Fig. 2.9 and highlight a good match with results presented in Fig. 2.8.

On comparing Fig. 2.8 and Fig. 2.9, it is evident that the obtained results (amplitude and phase modulation curves for the SLM) are in good agreement for both the conditions, viz. on a table top condition and in the presence of additional external vibrations. Availability of the complex fields of the orthogonal polarization components at the SLM plane permits to quantitatively evaluate the polarimetric phase $\phi_y - \phi_x$ and results are presented in Fig. 2.10. We have further tested and quantitatively compared these two results by determining root mean square error (RMSE) of polarimetric phase with respect to varying gray levels as shown in Fig. 2.10. The polarimetric phase represents the relative phase difference between the orthogonal field components E_x and E_y. The estimated RMSE of the relative phase for the two experimental cases (with a table top and with additional external vibrations) is 0.1661. The polarimetric parameters evaluated in this experiment are also compared with polarization holography setup designed in a controlled environment using the active vibration isolation table [75] and these results are in good agreement.

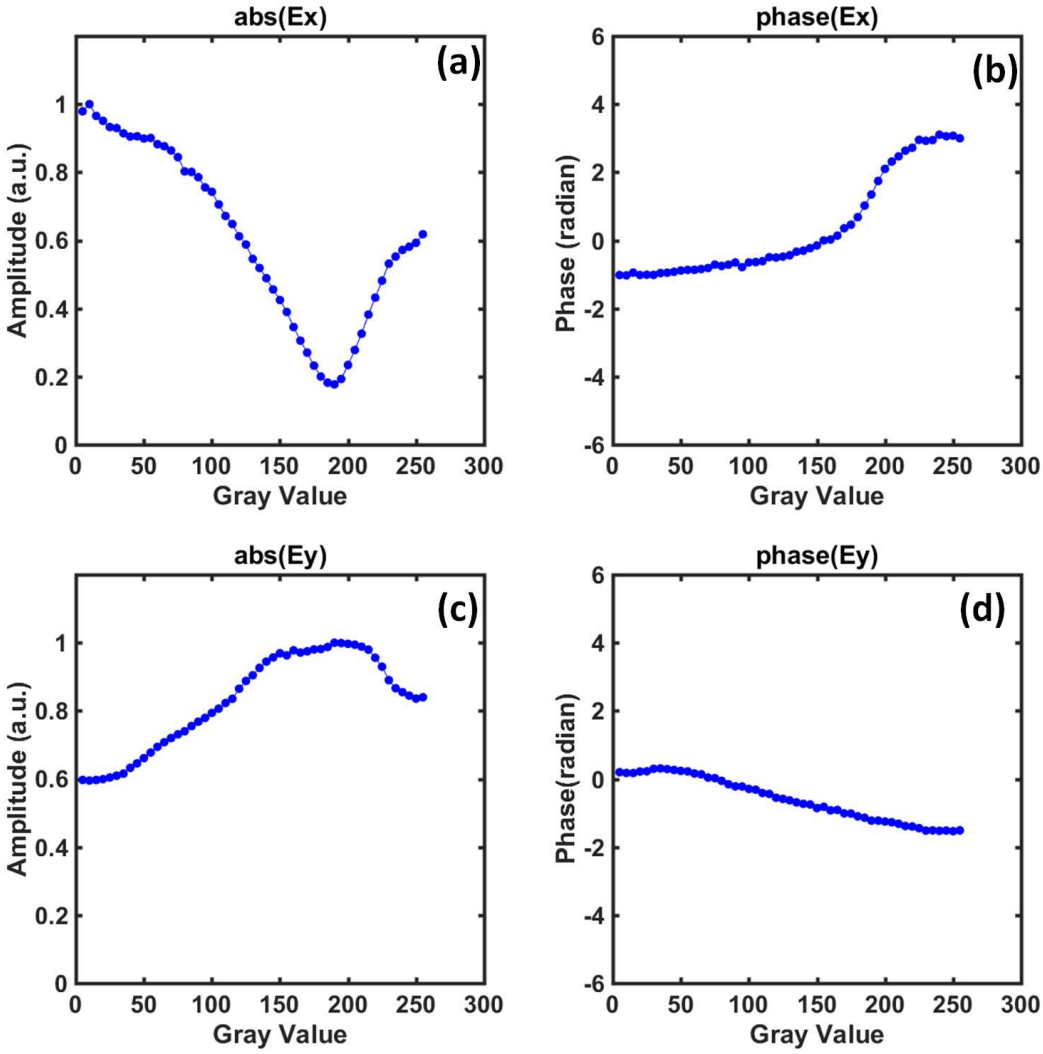

Fig. 2.9 Amplitude and phase modulation curve for incident 45 degree linearly polarized light in the presence of additional external vibrations,by placing a vibrating cell phone near to the setup. Amplitude and phase curve corresponding to field component E_x : (a) & (b); amplitude and phase curve corresponding to field component E_y : (c) & (d)

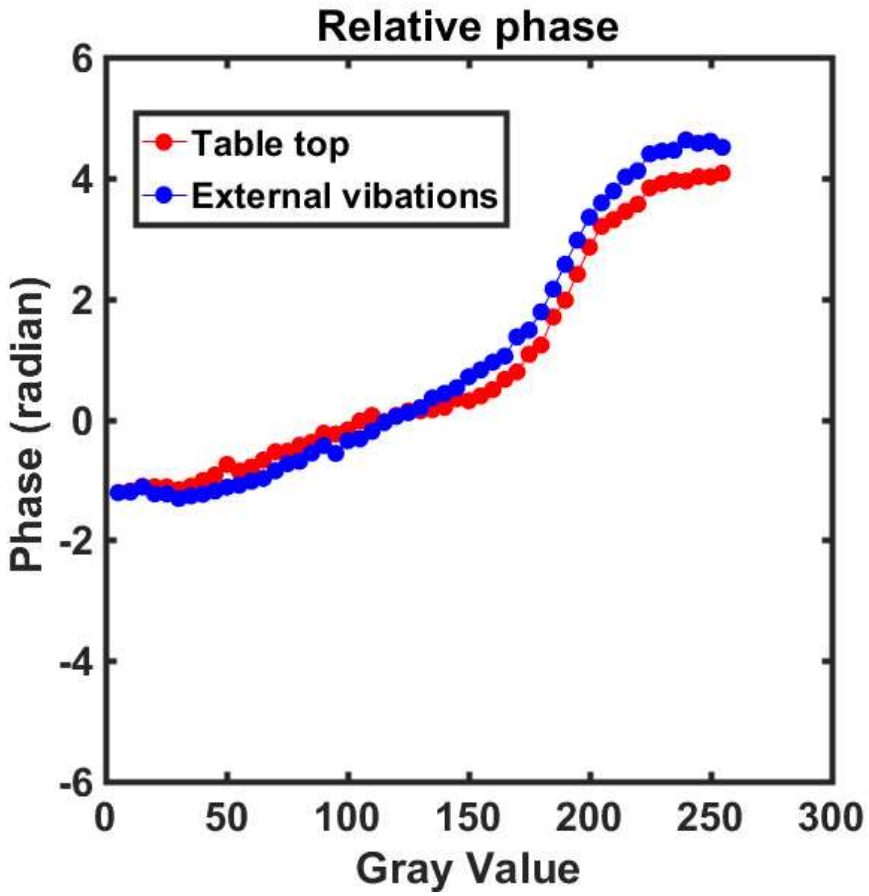

Fig. 2.10 Polarimetric phase of the electric field components using cyclic interferometric setup

2.4 Conclusion

In summary of this chapter, we present a new lens-less cyclic shearing interferometer system for polarimetric analysis of the SLM. The SLM modulations with the various gray levels are quantitatively evaluated by examining the orthogonal polarization components of the light reflecting from the SLM. Performance of this technique is experimentally tested in vibration isolation table and in presence of additional external vibrations. The results are in good agreement for both mentioned experimental conditions. In addition, present experimental system is compact and highly stable. Moreover, this technique

can be designed for single shot using polarization beam displacer to simultaneously record interferograms of the orthogonal polarization components. Our proposed technique is tolerant to external vibrations, thus is applicable in developing stable and compact polarimetric analysis schemes. Moreover, characterization results of the SLM with varying gray levels can also be used for different applications such as in coded aperture, light shaping and computer-generated hologram.